Accepted Manuscript

Identification of potent, selective and orally bioavailable phenyl ((*R*)-3-phenyl-pyrrolidin-3-yl)sulfone analogues as RORγt inverse agonists

Zhonghui Lu, James J.-W. Duan, Haiyun Xiao, James Neels, Dauh-Rurng Wu, Carolyn A. Weigelt, John S. Sack, Javed Khan, Max Ruzanov, Yongmi An, Melissa Yarde, Ananta Karmakar, Sureshbabu Vishwakrishnan, Venkata Baratam, Harisha Shankarappa, Sridhar Vanteru, Venkatesh Babu, Mushkin Basha, Arun Kumar Gupta, Selvakumar Kumaravel, Arvind Mathur, Qihong Zhao, Luisa M. Salter-Cid, Percy H. Carter, T.G. Murali Dhar

PII: S0960-894X(19)30416-0
DOI: https://doi.org/10.1016/j.bmcl.2019.06.036
Reference: BMCL 26514

To appear in: *Bioorganic & Medicinal Chemistry Letters*

Received Date: 11 April 2019
Revised Date: 11 June 2019
Accepted Date: 19 June 2019

Please cite this article as: Lu, Z., Duan, J.J., Xiao, H., Neels, J., Wu, D-R., Weigelt, C.A., Sack, J.S., Khan, J., Ruzanov, M., An, Y., Yarde, M., Karmakar, A., Vishwakrishnan, S., Baratam, V., Shankarappa, H., Vanteru, S., Babu, V., Basha, M., Kumar Gupta, A., Kumaravel, S., Mathur, A., Zhao, Q., Salter-Cid, L.M., Carter, P.H., Murali Dhar, T.G., Identification of potent, selective and orally bioavailable phenyl ((*R*)-3-phenylpyrrolidin-3-yl)sulfone analogues as RORγt inverse agonists, *Bioorganic & Medicinal Chemistry Letters* (2019), doi: https://doi.org/10.1016/j.bmcl.2019.06.036

ELSEVIER

Bioorganic & Medicinal Chemistry Letters
journal homepage: www.elsevier.com

Identification of potent, selective and orally bioavailable phenyl ((*R*)-3-phenylpyrrolidin-3-yl)sulfone analogues as RORγt inverse agonists

Zhonghui Lu*[a], James J.-W. Duan*[a], Haiyun Xiao[a], James Neels[a], Dauh-Rurng Wu[a], Carolyn A. Weigelt[a], John S. Sack[a], Javed Khan[a], Max Ruzanov[a], Yongmi An[a], Melissa Yarde[a], Ananta Karmakar[b], Sureshbabu Vishwakrishnan[b], Venkata Baratam[b], Harisha Shankarappa[b], Sridhar Vanteru[b], Venkatesh Babu[b], Mushkin Basha[b], Arun Kumar Gupta[b], Selvakumar Kumaravel[b], Arvind Mathur[a], Qihong Zhao[a], Luisa M. Salter-Cid[a], Percy H. Carter[a] and T. G. Murali Dhar[a]

[a] *Research and Development, Bristol-Myers Squibb Company, Princeton, New Jersey 08543-4000, United States.*
[b] *Bristol-Myers Squibb-Biocon Research Center, Bangalore, India.*
* *Corresponding authors. E-mails: zhonghui.lu@bms.com, james.duan@bms.com*

ARTICLE INFO

Article history:
Received
Revised
Accepted
Available online

Keywords:
RORγt
Retinoic acid-related orphan receptor gamma t
Inverse agonist
Th17
IL-17

ABSTRACT

An X-ray crystal of one of our previously discovered RORγt inverse agonists bound to the RORγt ligand binding domain revealed that the cyclohexane carboxylic acid group of compound **2** plays a significant role in RORγt binding, forming four hydrogen bonding and ionic interactions with RORγt. SAR studies centered around the cyclohexane carboxylic acid group led to identification of several structurally diverse and more potent compounds, including new carboxylic acid analogues **7** and **20**, and cyclic sulfone analogues **34** and **37**. Notably, compounds **7** and **20** were found to maintain the desirable pharmacokinetic profile of **2**.

The retinoic acid-related orphan receptor (ROR) family of nuclear receptors comprises three members: RORα, RORβ and RORγ (RORγt being a splice variant of RORγ).[1] The three RORs share a high degree of sequence similarity, but exhibit distinct tissue distribution patterns and distinct functional roles in the regulation of many physiological processes including development, immunity, circadian rhythm and cellular metabolism.[2] RORγt is the key transcription factor that drives differentiation of naïve $CD4^+$ T helper cells to Th17 cells, and induces the transcription of IL-17A and IL-17F.[3] There is abundant evidence that the IL-17/Th17 pathway plays an important role in the pathogenesis of psoriasis.[4] Biologics known to inhibit the IL-17/Th17 pathway are clinically validated for the treatment of psoriasis.[5] Targeting RORγt also provides a novel opportunity to treat other autoimmune diseases such as inflammatory bowel disease (IBD), rheumatoid arthritis (RA) and multiple sclerosis (MS).[6] In addition, RORγt-deficient mice show significantly reduced Th17 cell populations and decreased susceptibility to experimental autoimmune encephalomyelitis (EAE) as well as intestinal and skin inflammation.[1,7] Thus RORγt has garnered significant attention as a small molecule therapeutic target.[8-12]

Our group recently reported the discovery of a series of bicyclic sulfonamides as RORγt inverse agonists.[13] A representative compound **1** (Figure 1) showed an EC_{50} of 39 nM in the Jurkat cell-based Gal4 reporter assay for RORγt. However, it suffered from agonist activity against pregnant X receptor (PXR) *in vitro* (EC_{50} = 2000 nM, Y_{max} = 100%) and cytochrome P450 induction *in vivo*. We then described structure-based drug design efforts that led to a novel phenyl (3-phenylpyrrolidin-3-yl)sulfone series as exemplified by compound **2** (Figure 1).[14] Compound **2** exhibited an EC_{50} of 119 nM in the RORγt Gal4 reporter assay, no detectable activity against PXR and desirable pharmacokinetic (PK) profiles in mouse. Furthermore, compound **2** displayed dose-dependent inhibition of IL-17 production in a mouse IL-2/IL-23-induced pharmacodynamic model and biologic-like efficacy in an IL-23-induced mouse acanthosis model. This letter describes subsequent structure-activity relationship (SAR) studies to improve the potency of compound **2**.

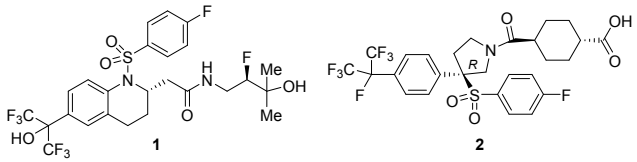

RORγt EC_{50} = 39 ± 18 nM
PXR EC_{50} = 2000 nM (100% max)

RORγt EC_{50} = 119 ± 28 nM
PXR EC_{50} = >50000 nM (18% max)

Figure 1. Previously reported RORγt inverse agonists.

Previous SAR studies[14] of the phenyl (3-phenylpyrrolidin-3-yl)sulfone scaffold revealed that the (*R*)-enantiomer of the pyrrolidine was more potent than the (*S*)-enantiomer; the perfluoroisopropyl and *para*-fluorophenyl groups were optimal for balanced potency-selectivity profiles; and the *trans*-cyclohexane stereochemistry in compound **2** provided greater potency than the *cis*-isomer. To gain insights on how to improve potency, an X-ray crystal structure of compound **2** with the ligand binding domain (LBD) of RORγt was solved (Figure 2).[15] Compared to a previously disclosed structure of a related analogue (compound **12** in ref. 14), the phenyl (3-phenylpyrrolidin-3-yl)sulfone backbone of **2** adopted a similar binding mode in RORγt. The *trans*-cyclohexane ring adopted a chair conformation, placing the two carbonyl groups in a 1,4-di-equatorial arrangement. The terminal carboxylic acid moiety fits nicely in a binding site surrounded by multiple polar amino acid residues - forming four polar (hydrogen bonding and ionic) interactions with backbone NH groups of Gln286 and Leu287 and guanidine side chains of Arg364 and Arg367.

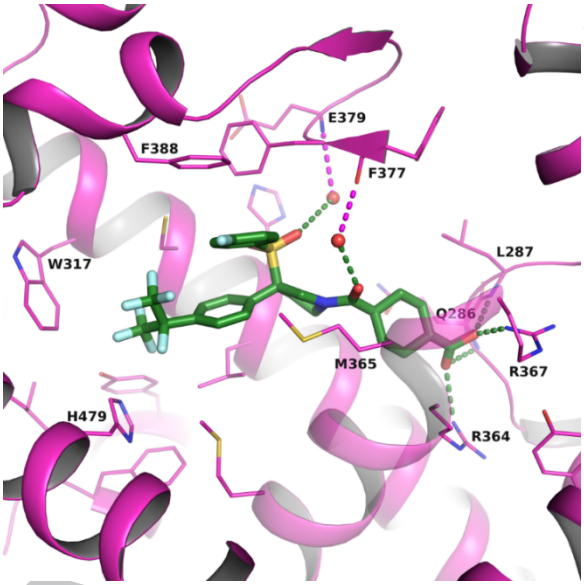

Figure 2. X-ray crystal structure of compound **2** and the LBD of RORγt (PDB ID 6P9F). The carbons of the protein are colored in pink and those of **2** in green. Sulfurs are colored in yellow, nitrogens in blue, oxygens in red and fluorines in cyan. Hydrogen bonds between compound **2** and RORγt LBD are indicated by a dashed line.

The carboxylic acid moiety of **2** not only engages multiple hydrogen bonding interactions with the RORγt LBD, but also improves metabolic stability of the series. Therefore, part of our SAR optimization efforts was to keep the carboxylic acid group intact and explore additional substitution to the cyclohexane ring in order to improve RORγt potency. We also envisioned that rigidification of the cyclohexane ring with fused/bridged bicyclic scaffolds, while maintaining the two carbonyl groups close to the 1,4-di-equatorial orientation, could lead to potency improvements. In parallel, we also explored structural diversity by investigating alternative functional groups to the carboxylic acid, because of the potential liability of the carboxylic acid group toward glucuronidation.

The effects of additional substitution to 1- and 4-position of the cyclohexane ring (α to the carboxylic acid and the carboxamide, respectively) are summarized in Table 1. The *trans*-1-methyl cyclohexane carboxylic acid **3** was perhaps more active than compound **2** (EC_{50} of 79 nM *vs*. 119 nM). However, the *trans*-1-ethyl and 1-fluoro analogues (**4** and **5)** lost activity approximately 2 and 5 fold, respectively, compared to **2**. Substitution at 4-position of the cyclohexane ring turned out to be more fruitful. Alkyl-substituted *trans*-analogues (**6**-**8**) improved potency by 2-4 fold compared to **2**, with the ethyl derivative **7** being the most potent at 31 nM. The two ether compounds (**9** and **10**) were less potent compared to the alkyl analogues. Fluoro-substitution (**11**) was tolerated, whereas the two hydroxy analogues (**12** and **13**, *cis* or *trans* not assigned) were slightly less potent than **2**. Similar to previous observation[14], *cis*-cyclohexane carboxylic acids **14** and **15** showed much weaker activity compared to their *trans* counterparts (**5** and **6**, respectively). This could be explained by the fact that the *cis*-cyclohexanes in **14** and **15** cannot project the two carbonyl groups in the 1,4-di-equatorial orientation as observed in the structure of compound **2**/RORγt (Figure 2) and further demonstrated the importance of the di-equatorial conformation for binding affinity. Overall, analogues in Table 1 showed good selectivity against PXR and good liver microsome stability. Additionally, all compounds in Table 1 (as well as Tables 2 and 3) exhibited excellent selectivity against RORα (>40 μM), RORβ (>40 μM), LXRα (>7.5 μM) and LXRβ (>7.5 μM).

SAR related to the replacement of the cyclohexane ring with bicyclic scaffolds is outlined in Table 2. Three fused bicyclo[3.1.0]hexane analogues (**16**-**18**) were synthesized and were found to lose RORγt activity compared to **2**. Of the two bridged analogues, the bicyclo[2.2.2]octane compound **20** showed EC_{50} of 33 nM in the RORγt Gal4 reporter assay, while the corresponding bicyclo[2.2.1]heptane analogue **19** was about 10-fold less potent (392 nM). Also noteworthy here is that compound **20** maintained high selectivity against PXR and displayed promising liver microsome stability. Two oxabicyclo[2.2.2]octane analogues (**21** and **22**) were also prepared. Unfortunately, both of them lost potency by several fold compared to **20.** The enhanced potency of **20** compared to **2** could be explained by the ability of bicyclo[2.2.2]octane ring, a known bioisostere to the 1,4-*trans*-cyclohexane,[16] to place the two carbonyl groups in 180° arrangement, reminiscent of the 1,4-diequatorial binding conformation of **2** (figure 2). The added steric bulk of bicyclo[2.2.2]octane could also enhance binding to RORγt. In contrast, the bicyclo[2.2.1]heptane ring in **19** and the bicyclo[3.1.0]hexanes in **16**-**18** cannot effectively achieve the linear arrangement for the two carbonyl groups, thus leading to reduced RORγt potency.

Our efforts to identify non-carboxylic acid alternatives are summarized in Table 3. Compounds **23**-**31** were derived from direct replacement of the carboxylic acid group with known bioisosteres, while keeping the cyclohexane ring intact. Compared to the acid **2**, the tetrazole compound **23** showed significant loss of potency (~10 fold). Both isomers of hydantoin analogues (**24** and **25**) were also less potent than **2**. The potency loss for both tetrazole and hydantoins could be due to the fact that the increase steric bulk of these groups compared to the carboxylic acid cannot be accommodated by the small binding pocket of RORγt LBD. The amide **26** had comparable potency while the ester **27** showed much weaker activity as anticipated. Compound **28,** one of the two

Table 1. *In vitro* data of substituted cyclohexane carboxylic acid analogues

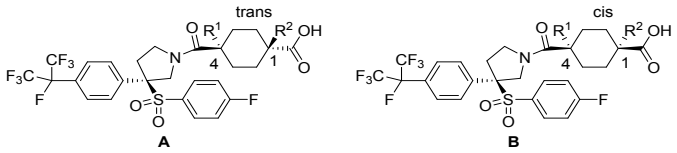

Cmpd #	Structure	R^1	R^2	RORγt EC_{50} nM[a,b]	PXR EC_{50} nM (% max.)[c]	LM (h, m) (% remaining)[d]
2	**A**	H	H	119 ± 28	>50000 (18)	97, 86
3	**A**	H	Me	79 ± 20	>50000 (18)	97, 93
4	**A**	H	Et	266 ± 119	>50000 (6)	100, -[e]
5	**A**	H	F	508 ± 152	>17000 (62)	100, 70
6	**A**	Me	H	56 ± 12	>50000 (7)	80, 95
7	**A**	Et	H	31 ± 24	>50000 (6)	89, 83
8	**A**	*n*-Pr	H	68 ± 37	-[e]	-[e], -[e]
9	**A**	MeO	H	594 ± 12	>18000 (94)	82, 95
10	**A**	$MeOCH_2$	H	109 ± 53	>50000 (7)	100, 88
11	**A**	F	H	74 ± 36	10600 (31)	-[e], -[e]
12	**A**	OH (isomer 1)	H	183 ± 67	>50000 (9)	100, 99
13	**A**	OH (isomer 2)	H	269 ± 40	>50000 (19)	95, 98
14	**B**	H	F	4177[c]	>22000 (69)	82, 94
15	**B**	Me	H	776[c]	>50000 (18)	85, 100

[a] Values are means of two or more experiments performed in duplicate unless otherwise noted. [b] RORγt reporter assay was performed using a Jurkat cell line. [c] Value from a single experiment performed in duplicate. [d] Metabolic stability in human and mouse liver microsome; values are percentage remaining after 10 min of incubation. [e] Not tested.

Table 2. *In vitro* data of bicyclic carboxylic acid analogues

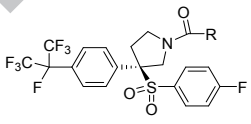

Cmpd #	R	RORγt EC_{50} nM[a,b]	PXR EC_{50} nM (% max.)[c]	LM (h, m) (% remaining)[d]
2	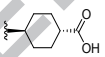	119 ± 28	>50000 (18)	97, 86
16	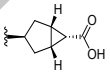	7295 ± 4358	>50000 (11)	100, 84
17	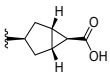	590[c]	>50000 (15)	100, -[e]
18	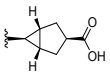	1480[c]	>33000 (43)	100, 100
19	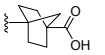	392[c]	-[e]	-[e], -[e]
20	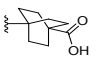	33 ± 11	>50000 (6)	100, 73
21	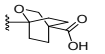	202 ± 62	>50000 (5)	90, 94
22	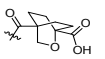	293 ± 139	>50000 (5)	-[e], -[e]

[a] Values are means of two or more experiments performed in duplicate unless otherwise noted. [b] RORγt reporter assay was performed using a Jurkat cell line. [c] Value from a single experiment performed in duplicate. [d] Metabolic stability in human and mouse liver microsome; values are percentage remaining after 10 min of incubation. [e] Not tested.

methyl sulfone isomers (*cis* or *trans* not assigned), exhibited similar potency to compound **2**. The primary alcohol **30** had respectful potency of 200 nM in Gal4 assay while the secondary alcohol **31** was notably less potent. Although several compounds showed comparable activity to **2** from this effort, no noticeable potency improvement was observed. Next set of compounds (**32-40**) represented analogues where the cyclohexane carboxylic acid moiety was replaced with cyclic sulfones. The five-membered cyclic sulfone isomers (**32** and **33**, absolute stereochemistry not assigned) had similar activity to **2**. It was exciting to find that the six-membered cyclic sulfone **34** improved RORγt potency to 33 nM. To our delight, it also displayed excellent metabolic stability and PXR selectivity. Thus substitution to the six-membered cyclic sulfone was pursued. Both methyl and ethyl analogues (**35** and **36**) lost potency by 2-3 fold compared to **34**. On the other hand, the fluoro analogue **37** maintained RORγt potency at 36 nM, good PXR selectivity and metabolic stability. Additional analogues with more polar hydroxy, hydroxymethyl and methoxy groups (**38-40,** respectively) resulted in reduced activity.

Table 3. *In vitro* data of non-carboxylic acid analogues

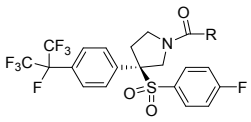

Cmpd #	R	RORγt EC_{50} nM[a,b]	PXR EC_{50} nM (% max.)[c]	LM (h, m) (% remaining)[d]
2	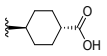	119 ± 28	>50000 (18)	97, 86
23	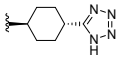	1260 ± 499	>50000 (11)	100, 73
24	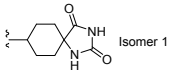	1900[c]	>14000 (28)	84, 81
25	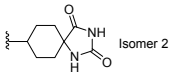	572[c]	>50000 (3)	93, 82
26	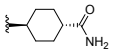	197 ± 140	>50000 (5)	100, 100
27	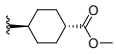	1167[c]	-[e]	-[e], -[e]
28	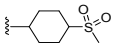	128 ± 56	1800 (29)	88, 69
29	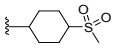	336 ± 106	>50000 (6)	100, -[e]
30	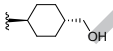	200 ± 107	>50000 (8)	75, 63
31		749 ± 290	>50000 (13)	86, 58
32	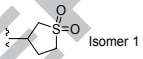	160 ± 22	>13000 (49)	100, 78
33	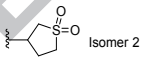	129 ± 94	7200 (37)	100, 96
34		33 ± 11	>50000 (5)	93, 96
35		102 ± 46	>50000 (10)	-[e], -[e]
36		83[c]	5200 (32)	3, 0
37		36 ± 8	>50000 (16)	100, 90
38		123 ± 60	>50000 (6)	100, 90
39		216 ± 120	>50000 (8)	75, 31
40		146 ± 24	>50000 (3)	-[e], -[e]

[a] Values are means of two or more experiments performed in duplicate unless otherwise noted. [b] RORγt reporter assay was performed using a Jurkat cell line. [c] Value from a single experiment performed in duplicate. [d] Metabolic stability in human and mouse liver microsome; values are percentage remaining after 10 min of incubation. [e] Not tested.

Compounds **7** and **20** were selected for further evaluation. Both compounds showed half-life of >120 min in the *in vitro* human, rat and mouse liver microsome stability assay. In a Caco-2 assay, both compounds **7** and **20** exhibited good permeability

(153 and 150 nm/s, respectively) and no detectable efflux (efflux ratio of 0.7 and 0.9, respectively). Compounds **7** and **20** were also found to have no significant CYP inhibition liabilities, with IC_{50} values greater than 10 μM against CYP1A2, 2B6, 2C8, 2C9, 2C19, 2D6 and 3A4. Because of their similar *in vitro* profiles, both compounds **7** and **20** were taken into mouse PK studies and the results were compared to compound **2** (Table 4). At an oral dose of 10 mg/kg, compound **7** displayed C_{max} of 3.7 μM and AUC (area under the curve) of 16.6 μM*h; and compound **20** achieved C_{max} of 6.7 μM and AUC of 24 μM*h which was comparable to compound **2.**

Table 4. PK profile of **7, 20** and **2** in balb/c mice[a]

Cmpd #	**7**	**20**	**2**
C_{max} (μM)	3.7	6.7	6.6
T_{max} (h)	0.5	1.0	2
AUC (μM*h)	16.6	24	36.6

[a] Oral dose: 10 mg/kg; vehicle: 5% *N*-methyl pyrrolidinone (NMP), 76% PEG 300, 19% TPGS.

Schemes 1-4 outline several representative synthesis. Scheme 1 illustrates the synthesis of compound **3**. Methylation of diester **41** gave the *cis*-isomer **42** as the only product. Epimerization of **42** with LDA deprotonation and methanol quenching followed by saponification provided the diacid **43** as a 1:1 mixture of *cis*- and *trans*-isomers. To facilitate separation of isomers, compound **43** was treated with oxalyl chloride followed by benzyl alcohol to yield the monobenzyl ester **44**. Separation of two isomers of **44** by chiral HPLC followed by hydrogenation gave the desired *trans*-diacid **45**. BOP-mediated coupling of **45** with intermediate **46**[14] completed the synthesis of **3**.

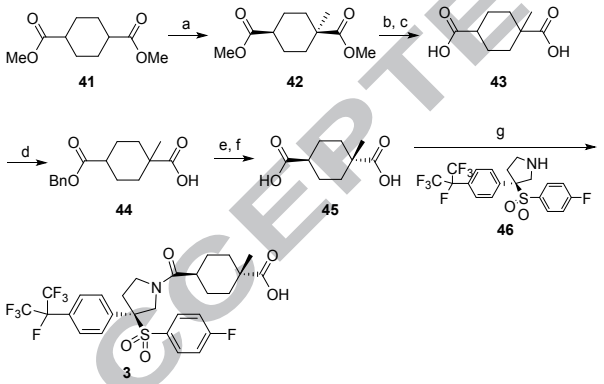

Scheme 1. Synthesis of **3**. Reagents and reaction conditions: (a) LDA, MeI, THF (78%); (b) LDA, THF, MeOH (83%, 1:1 mixture of *cis* and *trans* isomers); (c) LiOH, THF (94%); (d) $(COCl)_2$, DMF, BnOH, DCM (69%); (e) chiral OJ-H separation; (f) Pd/C, H_2, ethyl acetate (100%); (g) **46**, BOP, *i*-Pr_2NEt, DMF (54%).

Scheme 2 depicts the synthesis of compound **7**. *In situ* self-dimerization of **47** by treatment of triethylamine and mesyl chloride yielded **48**.[17] Ester-directed stereoselective hydrogenation of **48** with Crabtree's catalyst provided **49** as a single isomer. Treatment of **49** with DIBAL gave diol **50**. Oxidation of **50** using freshly prepared chromic acid solution followed by mono esterification produced **51**. BOP-mediated coupling of **51** with **46** followed by deprotection provided **7**.

Scheme 3 shows the synthesis of compounds **16** and **17**. Treatment of the acid **52** with $(Boc)_2O$ and DMAP in *tert*-butanol gave the *tert*-butyl ester **53**. Cyclopropanation of **53** with ethyl diazoacetate was achieved using rhodium (II) acetate dimer as a catalyst in dichloromethane yielded a 1:5 mixture of **54** and **55**.[18] After separation of two isomers, deprotection of each compound with TFA followed by HATU-mediated coupling with **46** and saponification provided **16** and **17**.

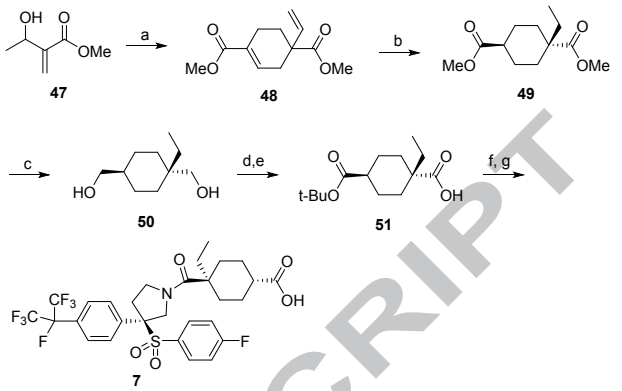

Scheme 2. Synthesis of **7**. Reagents and reaction conditions: (a) TEA, MsCl, DCM (40%); (b) H_2, Crabtree's catalyst, DCM (98%); (c) DIBAL, toluene, -78 ºC (99%); (d) H_2CrO_4, acetone, water (67%); (e) $(Boc)_2O$, DMAP, *t*-BuOH (40%); (f) **46**, BOP, *i*-Pr_2NEt, DMF (69%); (g) TFA, DCM (83%).

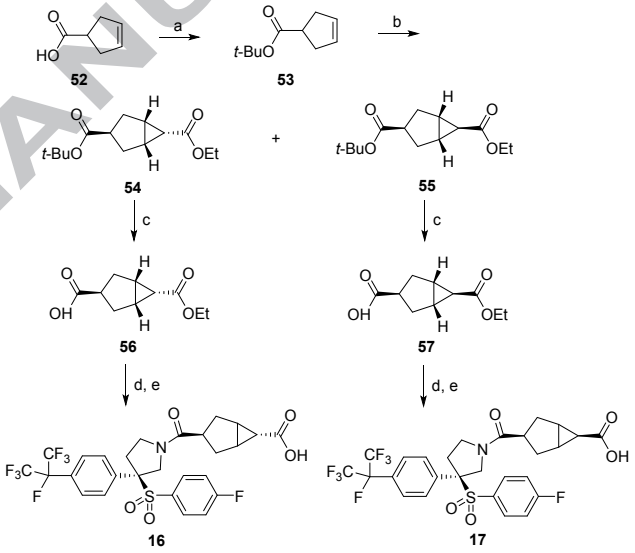

Scheme 3. Synthesis of **16** and **17**. Reagents and reaction conditions: (a) $(Boc)_2O$, DMAP, *t*-BuOH (67%); (b) ethyl diazoacetate, $Rh_2(OAc)_4$, DCM (50%); (c) TFA, DCM; (d) **46**, HATU, *i*-Pr_2NEt, DMF; (e) LiOH, THF.

Scheme 4 describes the synthesis of compounds **21** and **22**. Treatment of ethyl acrylate (**58**) and two equivalents of diethyl malonate (**59**) with sodium hydride in THF provided compound **60**. Decarboxylation of **60** followed by protection of the ketone yielded compound **61**. LAH reduction of **61** gave the diol **62**. Conversion of the diol to *bis*-tosylate followed by ketal deprotection delivered **63**. Grignard addition to the ketone **63** followed by cyclization produced **64**. Conversion of the tosylate to the acetate followed by hydrolysis provided the alcohol **65**. Oxidation of **65** followed by esterification gave **66**. Ozonolysis of **66** followed by oxidation yielded the acid **67**. HATU-mediated coupling of **67** with **46** followed by hydrogenation completed the synthesis of **21**. Alternatively, esterification of **67** followed by hydrogenation gave the acid **68**. Coupling of **68** with **46** followed by hydrolysis completed the synthesis of **22**.

The rest of the compounds exemplified in this manuscript were prepared by BOP or HATU-mediated coupling of the common intermediate **46** with the corresponding carboxylic acid side chain.

In summary, detailed SAR studies around the cyclohexane carboxylic acid moiety of compound **2** were carried out. Compounds **7**, **20**, **34** and **37** all improved RORγt inverse agonist potency by several fold compared to **2**. Furthermore, compounds **7** and **20** were found to essentially maintain the desirable pharmacokinetic profile of **2**. Compounds **34** and **37** represent non-carboxylic acid alternatives with improved potency. The combination of improved potency, good PK profile and structure diversity of these new side chains represents significant progress in the SAR development of the phenyl ((*R*)-3-phenylpyrrolidin-3-yl)sulfone series of RORγt inverse agonists. Application of these findings with new core modifications to further improve potency will be reported in the future.

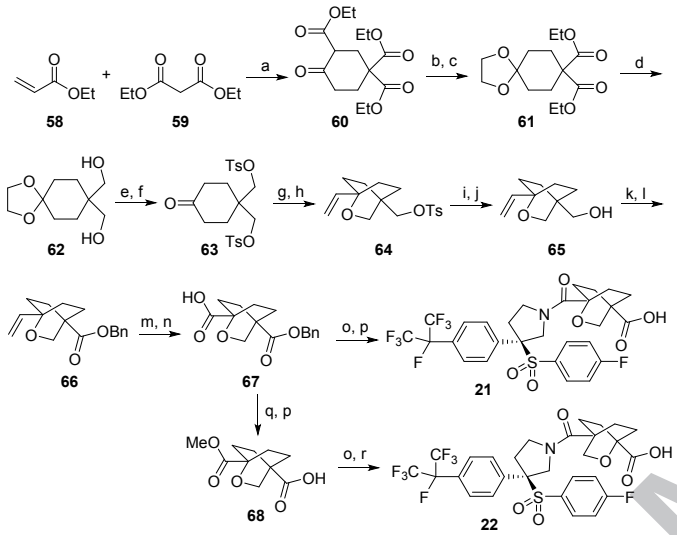

Scheme 4. Synthesis of **21** and **22**. Reagents and reaction conditions: (a) NaH, THF (51%); (b) NaCl, DMSO, H_2O, 160 ºC (88%); (c) ethylene glycol, TsOH, toluene, reflux (85%); (d) LAH, Et_2O, 0 ºC (74%); (e) TsCl, pyridine (90%); (f) HCl, THF, reflux (94%); (g) vinylmagnesium bromide, THF, -78 ºC; (h) NaH, DME, reflux (55% for two steps); (i) CsOAc, DMF, 100 ºC (97%); (j) K_2CO_3, MeOH, H_2O (94%); (k) PDC, DMF; (l) BnBr, K_2CO_3, DMF (72% for two steps); (m) O_3, DCM, Me_2S, -78 ºC; (n) $NaClO_2$, 2-methylbut-2-ene, NaH_2PO_4, H_2O, *t*-BuOH (85% for two steps); (o) **46**, HATU, *i*-Pr_2NEt, DMF; (p) H_2, MeOH; (q) $TMSCH_2N_2$, MeOH, toluene; (r) LiOH, THF.

Acknowledgments

We would like to thank Dr. Robert Borzilleri for critical review of the manuscript.

References and notes

1. Jetten, A. M. *Nucl. Recept. Signal*. **2009**, *7*, e003.
2. Cook, D. N.; Kang, H. S.; Jetten, A. M. *Nucl. Receptor Res*. **2015**, *2*, Article ID 101185.
3. Ivanov, I. I.; McKenzie, B. S.; Zhou, L.; Tadokoro, C. E.; Lepelley, A.; Lafaille, J. J.; Cua, D. J.; Littman, D. R. *Cell* **2006**, *126*, 1121.
4. Elloso, M. M.; Gomez-Angelats, M.; Fourie, A. M. *J. Leukoc. Biol.* **2012**, *92*, 1187.
5. Rizvi, S.; Chaudhari, K.; Syed, B. A. *Nat. Rev. Drug Discov*. **2015**, *14*, 745.
6. (a) Chabaud, M.; Durand, J. M.; Buchs, N.; Fossiez, F.; Page, G.; Frappart, L.; Miossec, P. *Arthritis Rheum*. **1999**, *42*, 963. (b) Lock, C.; Hermans, G.; Pedotti, R.; Brendolan, A.; Schadt, E.; Garren, H.; Langer-Gould, A.; Strober, S.; Cannella, B.; Allard, J.; Klonowski, P.; Austin, A.; Lad, N.; Kaminski, N.; Galli, S. J.; Oksenberg, J. R.; Raine, C. S.; Heller, R.; Steinman, L. *Nat. Med*. **2002**, *8*, 500. (c) Seiderer, J.; Elben, I.; Diegelmann, J.; Glas, J.; Stallhofer, J.; Tillack, C.; Pfennig, S.; Jürgens, M.; Schmechel, S.; Konrad, A.; Göke, B.; Ochsenkühn, T.; Müller-Myhsok, B.; Lohse, P.; Brand, S. *Inflamm. Bowel Dis*. **2008**, *14*, 437.
7. (a) Withers, D. R.; Hepworth, M. R.; Wang, X.; Mackley, E. C.; Halford, E. E.; Dutton, E. E.; Marriott, C. L.; Brucklacher-Waldert, V.; Veldhoen, M.; Kelsen, J. *Nat Med*. **2016**, *22*, 319. (b) Xue, X.; Soroosh, P.; De Leon-Tabaldo, A.; Luna-Roman, R.; Sablad, M.; Rozenkrants, N.; Yu, J.; Castro, G.; Banie, H.; Fung-Leung, W. P. *Sci. Rep*. **2016**, *6*, 37977.
8. Dhar, T. G. M.; Zhao, Q.; Markby, D. W. *Annu. Rep. Med. Chem.* **2013**, *48*, 169.
9. Cyr, P.; Bronner, S. M.; Crawford, J. J. *Bioorg. Med. Chem. Lett*. **2016**, *26*, 4387.
10. Fauber, B. P.; Magnuson, S. *J. Med. Chem.* **2014**, *57*, 5871.
11. Kojetin, D. J.; Burris, T. P. *Nat. Rev. Drug Discov*. **2014**, *13*, 197.
12. Pandya, V. B.; Kumar, S.; Sachchidanand, S.; Sharma, R.; Desai, R. C. *J. Med. Chem.* **2018**, *61*, 10976.
13. Gong, H.; Weinstein, D. S.; Lu, Z.; Duan, J. J.-W.; Stachura, S.; Haque, L.; Karmakar, A.; Hemagiri, H.; Raut, D. K.; Gupta, A. K.; Khan, J.; Camac, D.; Sack, J. S.; Pudzianowski, A.; Wu, D.-R.; Yarde, M.; Shen, D.-R.; Borowski, V.; Xie, J. H.; Sun, H.; D'Arienzo, C.; Dabros, M.; Galella, M. A.; Wang, F.; Weigelt, C. A.; Zhao, Q.; Foster, W.; Somerville, J. E.; Salter-Cid, L. M.; Barrish, J. C.; Carter, P. H.; Dhar, T. G. M. *Bioorg. Med. Chem. Lett.* **2018**, *28*, 85.
14. Duan, J. J.-W.; Lu, Z.; Jiang, B.; Stachura, S.; Weigelt, C. A.; Sack, J. S.; Khan, J.; Ruzanov, M.; Galella, M. A.; Wu, D.-R.; Yarde, M.; Shen, D.-R.; Shuster, D. J.; Borowski, V.; Xie, J. H.; Zhang, J.; Vanteru, S.; Gupta, A. K.; Mathur, A.; Zhao, Q.; Foster, W.; Salter-Cid, L. M.; Carter, P. H.; Dhar, T. G. M. *ACS Med. Chem. Lett*. **2019**, *10*, 367.
15. Attempts to obtain a structure of compound **2** with RORγt LBD using the same protein as reported in references 13 and 14 were unsuccessful. Therefore, a new RORγt LBD construct was used for the co-crystal structure of compound **2**. The new construct differs from the previous one in that the protein was covalently linked to a SRC1 peptide which was found to help co-crystallization. Details about the modified protein can be found in the deposited structure (PDB ID 6P9F).
16. (a) Kiesman, W. F.; Zhao, J.; Conlon, P. R.; Dowling, J. E.; Petter, R. C.; Lutterodt, F.; Jin, X.; Smits, G.; Fure, M.; Jayaraj, A.; Kim, J.; Sullivan, G.; Linden, J. *J. Med. Chem*. **2006**, *49*, 7119. (b) Barlind, J. G.; Bauer, U. A.; Birch, A. M.; Birtles, S.; Buckett, L. K.; Butlin, R. J.; Davies, R. D. M.; Eriksson, J. W.; Hammond, C. D.; Hovland, R.; Johannesson, P.; Johansson, M. J.; Kemmitt, P. D.; Lindmark, B. T.; Gutierrez, P. M.; Noeske, T. A.; Nordin, A.; O'Donnell, C. J.; Petersson, A. U.; Redzic, A.; Turnbull, A. V.; Vinblad, J. *J. Med. Chem*. **2012**, *55*, 10610. (c) Zhong, M.; Peng, E.; Huang, N.; Huang, Q.; Huq, A.; Lau, M.; Colonno, R.; Li, L. . *Bioorg. Med. Chem. Lett.* **2014**, *24*, 5731.
17. Rensburg, D. J. V.; Mason, P. H.; Emslie, N. D. *Synth. Commun.* **1996**, *26*, 4403.
18. Kozhushkov, S. I.; Langer, R.; Yufit, D. S.; Howard, J. A. K.; Schill, H.; Demus, D.; Miyazawa, K.; Meijere, A. D. *Eur. J. Org. Chem.* **2004**, *2*, 289.

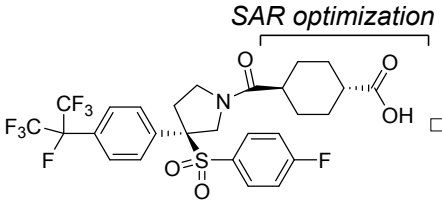

2

RORγt EC_{50} = 119 nM

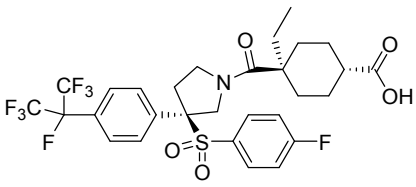

7

RORγt EC_{50} = 31 nM

Orally bioavailable in mouse

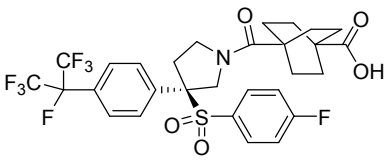

20

RORγt EC_{50} = 33 nM

Orally bioavailable in mouse

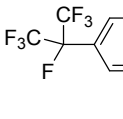

ROR

19.